



**HAL**  
open science

## On the resolution of the isotropic component in moment tensor inversion

H. Dufumier, Luis Rivera

► **To cite this version:**

H. Dufumier, Luis Rivera. On the resolution of the isotropic component in moment tensor inversion. *Geophysical Journal International*, 1997, 131 (3), pp.595-606. 10.1111/j.1365-246X.1997.tb06601.x . hal-03258835

**HAL Id: hal-03258835**

**<https://hal.science/hal-03258835>**

Submitted on 14 Jun 2021

**HAL** is a multi-disciplinary open access archive for the deposit and dissemination of scientific research documents, whether they are published or not. The documents may come from teaching and research institutions in France or abroad, or from public or private research centers.

L'archive ouverte pluridisciplinaire **HAL**, est destinée au dépôt et à la diffusion de documents scientifiques de niveau recherche, publiés ou non, émanant des établissements d'enseignement et de recherche français ou étrangers, des laboratoires publics ou privés.

# On the resolution of the isotropic component in moment tensor inversion

H. Dufumier and L. Rivera

Institut de Physique du Globe, 5 rue R. Descartes, 67084 Strasbourg Cedex, France. E-mail: hugues@sismo.u-strasbg.fr; luis@sismo.u-strasbg.fr

Accepted 1997 June 24. Received 1997 June 23; in original form 1996 July 8

## SUMMARY

It is in theory possible to solve a full moment tensor from inversion of a few seismograms, using normal-mode data, surface waves or body waves. In fact, the isotropic component is usually set to zero in many inversions, in order to stabilize them. This approximation may be considered valid for tectonic earthquakes, but for other applications (such as the study of nuclear or volcanic explosions, deep earthquakes and induced seismicity), the determination of the volumetric component is a key point of the inversion. Our aim is to investigate under which practical conditions the determination of the isotropic component is feasible, and is mathematically and physically reliable. In the first part, we examine the question from a physical point of view and show that the classical interpretation of a full moment tensor for tectonic events implies rheological constraints that are not always realistic. We therefore propose an extended physical model which includes tectonic and non-tectonic volumetric variations. In the second part, we use the tools of inverse theory to infer mathematical constraints on the problem of full moment tensor inversions, from teleseismic surface-wave or body-wave spectra. In particular, we examine how much of the moment tensor can be solved, in relation to the eigenvalues, the condition number and the sampling of the inverse problem. In addition, the resolution and the correlation matrices show that, among a choice of possible constraints on the full tensor, a constraint on the isotropic component is most valuable. In the third part, we also show some applications of our theoretical developments to regional waveform inversions, using the 1992 April Roermond, the Netherlands, earthquake. In addition to physically reliable estimations of the tectonic and non-tectonic isotropic components in full moment tensor inversions, we finally propose extensions of the basic linear methods that can lead to particular models in subspaces of interest, such as tectonic models, or decompositions in a double-couple plus a volumetric part. By revisiting carefully the determination and interpretation of moment tensors, we provide new perspectives in the estimation of the model and of its error, for a more flexible tectonic and physical interpretation of source mechanisms.

**Key words:** inverse problem, isotropic component, moment tensor.

## 1 INTRODUCTION

The linear relation between the six elements of a symmetric moment tensor and waveforms (or spectra) has been extensively used to invert directly the source mechanism from a set of seismograms [see Jost & Herrmann (1989) for a review of the techniques]. For example, moment tensor inversions of surface-wave spectra or of normal modes can be described by system (1), and teleseismic body-wave moment tensor inversions, using the ray theory, by system (2). Both systems are presented in their simplest forms, linking the radiation

spectra  $\mathfrak{R}$  to combinations of the moment tensor elements  $M_{ij}$  which are common to surface waves and body waves (Kanamori & Stewart 1976; Dufumier 1996; Kawakatsu 1996). We have

$$\begin{aligned}\mathfrak{R}_{\text{Rayl.V}} &= -kr_1(p_R + s_R) - i(r'_1 - kr_2)q_R + 2r'_2s_R, \\ \mathfrak{R}_{\text{Rayl.L}} &= -i(-kr_1(p_R + s_R) - i(r'_1 - kr_2)q_R + 2r'_2s_R), \\ \mathfrak{R}_{\text{Love}} &= -ikl_1p_L + l'_1q_L,\end{aligned}\tag{1}$$

where  $k$  is the wavenumber and  $r_1, r_2, l_1, r'_1, r'_2, l'_1$  are the eigenfunctions and their derivatives at the source depth  $h$ , as

defined in Aki & Richards (1980), and

$$\begin{aligned}\mathfrak{R}_p &= -\sin^2(i_h)(p_R + s_R) - \sin(2i_h)q_R + 2\cos^2(i_h)s_R, \\ \mathfrak{R}_{sv} &= -\frac{1}{2}\sin(2j_h)(p_R + s_R) - \cos(2j_h)q_R - \sin(2j_h)s_R,\end{aligned}\quad (2)$$

$$\mathfrak{R}_{SH} = \sin(j_h)p_L + \cos(j_h)q_L,$$

where  $i_h$  and  $j_h$  are the respective incidence angles of  $P$  and  $S$  waves at the hypocentre. Depending on the distances used, these radiation spectra should also include the contribution of the reflected phases, considering their reflection coefficients and phase delays.

Here,  $p_R$ ,  $q_R$ ,  $s_R$ ,  $p_L$  and  $q_L$  are linear combinations of the moment tensor elements  $M_{ij}$ , with coefficients depending on the station azimuth  $\phi$ , as defined in Kanamori & Stewart (1976):

$$\begin{aligned}M_0 p_R &= -\cos^2\phi M_{xx} - \sin(2\phi)M_{xy} - \sin^2\phi M_{yy} - M_{zz}/2, \\ M_0 q_R &= -\cos\phi M_{xz} - \sin\phi M_{yz}, \\ M_0 s_R &= M_{zz}/2, \\ M_0 p_L &= \sin\phi \cos\phi(M_{yy} - M_{xx}) + \cos(2\phi)M_{xy}, \\ M_0 q_L &= \cos\phi M_{yz} - \sin\phi M_{xz}.\end{aligned}\quad (3)$$

We use here the orientation and sign conventions of Aki & Richards (1980),  $x$ ,  $y$  and  $z$  denote, respectively, the north, east and downward axes, and the station azimuth  $\phi$  is measured clockwise from the north.

In theory, the five elements  $p_R$ ,  $q_R$ ,  $s_R$ ,  $p_L$  and  $q_L$  can be solved from a single-station inversion, but to solve the six components of the moment tensor, at least two three-component stations are needed. In practice, more stations are needed, and an additional constraint is often applied in order to stabilize the system, by setting the isotropic component to zero:

$$M_{xx} + M_{yy} + M_{zz} = 0.$$

This constraint is convenient for seismological applications when the earthquake source mechanism is supposed to match a dislocation model inside a fault plane. For more general applications, however, this approximation might not be appropriate. For example, Foulger & Long (1984) study tensile crack formations associated with small seismic events in a geothermal field; Campus *et al.* (1996) are interested in point-source full moment tensor inversions in volcanic areas; Ekström & Richards (1994) and Wu & Chen (1996) analyse the parts of explosion and tectonic strain release in nuclear explosions; while Kawakatsu (1996) and Hara, Kuge & Kawakatsu (1996) examine the observability of the isotropic component of deep earthquakes. Even for tectonic earthquakes, the double-couple assumption of a slip direction purely parallel to the fault plane might be approximative.

Our aim is to investigate under which practical conditions the determination of the isotropic component is mathematically and physically reliable. We treat these questions following a rather tutorial scheme, complemented by some illustrative applications referring to various moment tensor inversion methods. In the first part, we examine the question from a physical point of view. First, we discuss the general physical description of a moment tensor for tectonic events and its limitations. Then, we propose an extended model which includes possible non-tectonic volumetric variations. In the second part, we use the tools of inverse theory in order to infer mathematical constraints on the resolution of the moment

tensor from teleseismic surface wave or body-wave spectra. In the third part, we also show some application of our theoretical developments to regional waveform inversions. We finally propose adaptations of the methods that can lead to reliable estimations of the tectonic and non-tectonic isotropic components, or of particular models of interest.

## 2 PHYSICAL CONSTRAINTS ON THE DESCRIPTION OF A MOMENT TENSOR

### 2.1 Classical description of a moment tensor for a tectonic event

In earthquake seismology, a generalized seismic source is usually described by a model of a fault plane with a slip vector  $\mathbf{s}$  that might be out of the fault plane (Fig. 1). This model is rather appealing because of its simple geometric interpretation, but it is not as general as a full symmetric moment tensor and, additionally, it introduces artificial coupling between the rheological parameters  $\lambda$  and  $\mu$ .

In order to develop this argument, let us denote as  $\mathbf{n}$  the normal to the fault plane, oriented outwards,  $\alpha$  the angle between  $\mathbf{n}$  and  $\mathbf{s}$ , and  $\boldsymbol{\tau}$  the projection of  $\mathbf{s}$  onto the fault plane. The case  $\alpha < 90^\circ$  ( $\cos\alpha > 0$ ) corresponds to a mechanism in extension,  $\alpha > 90^\circ$  ( $\cos\alpha < 0$ ) to a compression, and  $\cos\alpha = 0$  to a pure double-couple. Then

$$\mathbf{s} = \cos\alpha\mathbf{n} + \sin\alpha\boldsymbol{\tau}.$$

We consider the vectors  $\mathbf{n}$ ,  $\boldsymbol{\tau}$  and  $\mathbf{s}$  to be unitary, and denote as  $S$  the area of the fault plane and  $D$  the extension of the slip vector. The general expression of a symmetric seismic moment tensor for a tectonic event is then (e.g. Aki & Richards 1980, p. 52; Udias 1991):

$$\mathbf{M} = \lambda SD(\mathbf{s} \cdot \mathbf{n})\mathbf{Id} + \mu SD(\mathbf{sn}^\perp + \mathbf{ns}^\perp), \quad (4)$$

where  $\cdot$  denotes the scalar product,  $^\perp$  the transposed, and  $\mathbf{Id}$  the identity tensor.

Therefore we obtain the following expression for  $\mathbf{M}$  in the reference frame  $\langle \boldsymbol{\tau}, \mathbf{n}, \boldsymbol{\tau} \wedge \mathbf{n} \rangle$ , where  $\wedge$  denotes the vectorial product:

$$\mathbf{M}_{\langle \boldsymbol{\tau}, \mathbf{n}, \boldsymbol{\tau} \wedge \mathbf{n} \rangle} = SD \begin{pmatrix} \lambda \cos\alpha & \mu \sin\alpha & 0 \\ \mu \sin\alpha & (\lambda + 2\mu) \cos\alpha & 0 \\ 0 & 0 & \lambda \cos\alpha \end{pmatrix}. \quad (5)$$

By diagonalization, we can deduce the expression of the

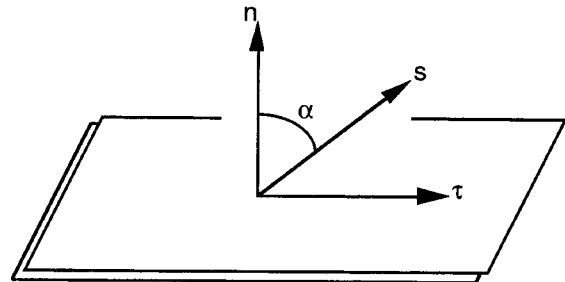


**Figure 1.** A classical model used to describe the non-double-couple mechanism of tectonic earthquakes. We denote  $\mathbf{n}$  the normal to the fault plane, oriented outwards,  $\mathbf{s}$  the slip vector,  $\boldsymbol{\tau}$  the projection of  $\mathbf{s}$  on the fault plane (all unitary vectors), and  $\alpha$  the angle between  $\mathbf{n}$  and  $\mathbf{s}$ .

moment tensor in the frame of the principal axes  $\langle P, N, T \rangle$ , which is more appropriate to decompose the tensor in submechanisms:

$$\mathbf{M}_{\langle P, N, T \rangle} = SD \begin{pmatrix} \lambda \cos \alpha + \mu(\cos \alpha - 1) & 0 & 0 \\ 0 & \lambda \cos \alpha & 0 \\ 0 & 0 & \lambda \cos \alpha + \mu(\cos \alpha + 1) \end{pmatrix}. \quad (6)$$

From this tensor are usually extracted uniquely the isotropic component  $I = (\lambda + 2\mu/3) \cos \alpha \mathbf{Id}$  and the complementary deviatoric part (e.g. Pearce & Rogers 1989; Jost & Herrmann 1989). A variety of decompositions of this type include the decomposition of the deviatoric part into two double-couples or into a double-couple plus a compensated linear vector dipole (e.g. Dziewonski, Chou & Woodhouse 1981; Jost & Herrmann 1989), or a physical diagram sketch of various possible sources (Pearce & Rogers 1989; Hudson, Pearce & Rogers 1989), or particular decompositions adapted to the study of deep earthquakes (Kawakatsu 1996).

The eigenvalues  $v_i$  of the full tensor (eq. 6) or the eigenvalues of the deviatoric tensor,  $v'_i = v_i - (v_1 + v_2 + v_3)/3$ , give a direct measure of some characteristics of the model, such as:

- (1) the 'global seismic moment' (Silver & Jordan 1982):

$$M_g = \sqrt{\frac{1}{2} \sum v_i^2};$$

- (2) the seismic moment of the best double-couple (Dziewonski *et al.* 1981):

$$M_0 = \frac{|v'_{\max}| + |v'_{\min}|}{2} = \mu SD;$$

- (3) the direction of the slip vector from the fault plane,

$$90^\circ - \alpha = \arcsin \left( 3 \frac{v'_{\max} + v'_{\min}}{v'_{\max} - v'_{\min}} \right);$$

or

- (4) the corresponding percentage of non-double-couple component in the deviatoric tensor (Dziewonski *et al.* 1981; Sipkin 1986; Kuge & Lay 1994a):

$$\varepsilon = \frac{|v'_{\min}|}{|v'_{\max}|} - \frac{2|\cos \alpha|}{3 + |\cos \alpha|}.$$

We might consider *a priori* that any six-component tensor can be described by the six parameters of the tectonic model of Fig. 1 and eq. (4). Indeed, there is a unique relation (eqs 5 and 6) between the six  $M_{ij}$  and the six parameters of the model:  $\lambda SD$ ,  $\mu SD$ ,  $\alpha$  and the three orientation parameters. But, in order to explain any moment tensor, the six physical parameters, in particular  $\lambda SD$  and  $\mu SD$ , should be independent. This implies that the ratio  $\lambda/\mu$  between the Lamé parameters would also be determined by the tensor

$$\frac{\lambda}{\mu} = \frac{\text{Trace}(\mathbf{M})}{\mu \cos \alpha} - \frac{2}{3} = \frac{2}{3} \left( \frac{\sum v_i}{v'_{\max} + v'_{\min}} - 1 \right). \quad (7)$$

For example, the tensor

$$\begin{pmatrix} -1 & 1 & 0 \\ 1 & 1 & 0 \\ 0 & 0 & -1 \end{pmatrix}_{\langle \tau, n, \tau \wedge n \rangle} = \begin{pmatrix} -\sqrt{2} & 0 & 0 \\ 0 & -1 & 0 \\ 0 & 0 & \sqrt{2} \end{pmatrix}_{\langle P, N, T \rangle}$$

corresponds to  $\alpha = 45^\circ$ , i.e. a double-couple of seismic moment  $M_0 = \sqrt{2}$ , plus  $\varepsilon = 38$  per cent of non-double-couple component, plus an implosive component  $M_{xx} + M_{yy} + M_{zz} = -1$ , but also to  $\lambda = -\mu$ , a rather non-physical constraint!

Another illustrative example is that, in such a model, a purely deviatoric tensor can correspond only to  $\lambda/\mu = -2/3$  or to a pure double-couple, and a pure explosion would correspond to an infinite ratio  $\lambda/\mu$ .

Generally, one considers that the rheological properties of the Earth are given and would not worry about their compatibility with the moment tensor. In this case, we should consider that the moment tensor has only five independent parameters. For example, if we consider the classical relation  $\lambda = \mu(V_P/V_S = \sqrt{3})$ , a given deviatoric tensor (which can be uniquely associated to  $\mu SD$ ,  $\alpha$  and three orientation parameters) would be necessarily flanked with an isotropic component  $M_{xx} + M_{yy} + M_{zz} = 5 \cos \alpha M_0$ . In this case, the isotropic component does not reflect a physical volumetric variation, but a limit of the tectonic model used to describe moment tensors.

Therefore, the tectonic interpretation of the full moment tensor obtained without the constraint of rheological plausibility has to face an alternative choice of constraints: either the solution must be constrained to be among the population of tensors described by five physically independent parameters, among which are the deviatoric moment tensors, but not the combinations of a double-couple plus a volumetric component (as can be easily seen from the model itself); or we need a model more sophisticated than the classical tectonic model described in Fig. 1. For example, Frolich, Riedersel & Apperson (1989) and Kuge & Lay (1994b) have related non double-couple parts to non-plane faults and inhomogeneous faults, respectively. Doornbos (1982) related first-degree moment tensors to 10 physical parameters, or second-degree moments to 20 source parameters. Other authors pointed out that the moment tensor is not appropriate to describe some indigenous sources (Kawakatsu 1989; Takei & Kumazawa 1994).

We will propose now a simple extension of the previous general tectonic model to non-tectonic or semi-tectonic phenomena.

## 2.2 Extended model including non-tectonic volumetric variations

The previous physical incompatibility between the rheological properties of the Earth and the observed volumetric component in a tectonic model may result from the fact that the compressional or extensional component reflects more a limitation of the model than a physical phenomenon. It is, in particular, inadequate to represent major implosive or explosive processes, fluid intrusions and, more generally, events that are not purely tectonic. In such a context, the addition of a purely implosive/explosive mechanism to the model seems natural. We therefore add to the previous general tectonic model a second isotropic component,  $E \mathbf{Id}$ , of non-tectonic nature ('E' standing, for

example, for 'explosion'):

$$\mathbf{M} = \lambda SD(\mathbf{s} \cdot \mathbf{n})\mathbf{Id} + \mu SD(\mathbf{sn}^\perp + \mathbf{ns}^\perp) + E \mathbf{Id}. \quad (8)$$

Any symmetric moment tensor can be described uniquely by the six independent parameters of this model, the two unitary (but not necessarily orthogonal) vectors  $\mathbf{n}$  and  $\mathbf{s}$ , the scalar moment  $M_0 = \mu SD$ , and an additional non-tectonic explosive/implosive component, without requiring undesirable physical assumptions on the Lamé parameters  $\lambda$  and  $\mu$ . In detail, the relations relating  $\mathbf{M}$  to  $\mathbf{n}$ ,  $\mathbf{s}$ ,  $SD$  and  $E$  are provided in Appendix A.

We are now able to model a wide range of processes, from the pure shear dislocation ( $\alpha = 90^\circ$ ,  $E = 0$ ) to pure explosions ( $SD = 0$ ), and including isotropic components of tectonic and/or explosive origin. We present here some particular applications of this model.

Concerning the interpretation of tectonic events, we note that the slip vector obtained with this model might differ from the one usually obtained by extraction of the 'best double-couple'. Being allowed to be off-fault, it may better fit a local stress field, acting on a given pre-existing fault plane.

Another application of this model, adapted to the description of fluid intrusion in geothermal exploitation, is the model of Foulger & Long (1984), including a tensile crack opening perpendicular to the fissure (i.e. the model of Fig. 1 with  $\mathbf{s} = \mathbf{n}$ , or  $\alpha = 0^\circ$ ), plus a pore pressure drop ( $E \mathbf{Id}$ ).

A general physical interpretation of nuclear events, equivalent to our model, is also given by Wu & Chen (1996). It is composed of the dominant explosive part ( $E \mathbf{Id}$ ) of the tectonic strain release (the double-couple part of our tectonic model) and of the spall, which includes a compensated linear vector dipole (Knopoff & Randall 1970) and the volumetric variation of a pre-existing tensional crack, i.e. the non-double-couple part of our tectonic model. They clearly fix the ratio  $\lambda/\mu$  from other observations, and therefore consider a physical model including two isotropic parts. They also show that if the trace of the observed tensor is kept as the only volumetric variation, both the assumed amplitude of the explosion and the geometry of the double-couple may be in error.

### 3 MATHEMATICAL CONSTRAINTS ON TELESEISMIC LINEAR MOMENT TENSOR INVERSIONS

We now present linear moment tensor inversions in their very general form; from here on,  $\mathbf{M}$  will represent a vector whose components are the six independent elements of the moment tensor:

$$\mathbf{D} = \mathbf{G}\mathbf{M},$$

where

$$\mathbf{M} = (M_{xx}, M_{xy}, M_{yy}, M_{xz}, M_{yz}, M_{zz}),$$

and we investigate the problem of the reliability of the tensor  $M_{ij}$ , using the tools of inverse theory.

Such a simple linear problem usually refers to long-period, teleseismic, moment tensor inversions, when the (non-linear) effects of hypocentral mislocation and rupture complexity can be considered of the second order. We illustrate our analysis using two methods, one based on the inversion of surface-wave spectra (Dufumier & Cara 1995) and the second based on body-wave spectra using the ray theory (Dufumier 1996).

The relation to the moment tensor being linear, the solution can be obtained by simple formulations of Lanczos' (1961) method, or, more classically, can be derived from the least-squares formalism

$$\mathbf{M} = (\mathbf{G}^t \mathbf{G})^{-1} \mathbf{G}^t \mathbf{D}. \quad (9)$$

#### 3.1 The conditioning

The discrepancy between what can be solved in theory from an inverse problem and what can be solved in practice is usually related to the stability of the inversion and can be illustrated by the system conditioning. The condition number, which can be computed before the inversion, and even from the direct problem, is defined as the ratio between the largest and smallest singular values of the matrix  $\mathbf{G}$  (e.g. Tarantola 1987):

$$\text{Cond} = \frac{\sup(\text{singular values}(\mathbf{G}))}{\inf(\text{singular values}(\mathbf{G}))} = \sqrt{\frac{\sup(\text{eigenvalues}(\mathbf{G}^t \mathbf{G}))}{\inf(\text{eigenvalues}(\mathbf{G}^t \mathbf{G}))}}.$$

A consequence is that the relative error  $e_m$  on the model may amount the relative error  $e_d$  on the data amplified by the condition number, and therefore the solution may become very unstable for high condition numbers (Menke 1989):

$$e_m \leq \text{Cond} \times e_d.$$

Long-period moment tensor inversions are known to be ill-conditioned, the reason coming either from the behaviour of  $M_{xz}$  and  $M_{yz}$  at shallow depths (Mendiguren 1977; Kanamori & Given 1981), from the poor resolution of  $M_{zz}$  (Fitch, North & Shields 1981), or from various trade-offs with other parameters (Fitch *et al.* 1981; Langston, Barker & Pavlin 1982; Satake 1985). Our practical experience with long-period data has shown that the inversion becomes strongly unstable for condition numbers greater than 5. This value may seem quite restrictive (a value of 10 is more usual), but can be understood by considering the fact that the relative standard error  $e_d$  on the observed spectra, measured comparing them with synthetics, is locally of a factor 2, i.e. of 200 per cent. Langston *et al.* (1982) also showed that, with a condition number of 10, the mechanism is very sensitive to the structure.

We have computed the condition numbers for the teleseismic body-wave and surface-wave problems, described respectively by Dufumier (1996) and Dufumier & Cara (1995). The frequency bandwidths used are of 10–60 s for body waves and 30–300 s for surface waves, as large as possible in order to optimize the condition number. Results are presented in Fig. 2 for different configurations of stations and components and for various depths. The value of the condition number is coded by a grey scale. On the left-hand side the result for full moment tensor inversions is shown, and on the right-hand side, inversions under the constraint  $M_{zz} = -M_{xx} - M_{yy}$  are shown.

It appears clearly that it is not possible to solve with confidence full moment tensors from teleseismic inversions, whatever the waves and the azimuthal aperture used. However, it is possible to retrieve stable deviatoric tensors using at least two three-component stations with a minimal azimuthal aperture of  $60^\circ$ . Even mechanisms of shallow earthquakes can be solved using body waves if the isotropic component is constrained to be null.

Note that the constraint  $M_{zz} = -M_{xx} - M_{yy}$  is not unique, even if it might be considered as a good choice

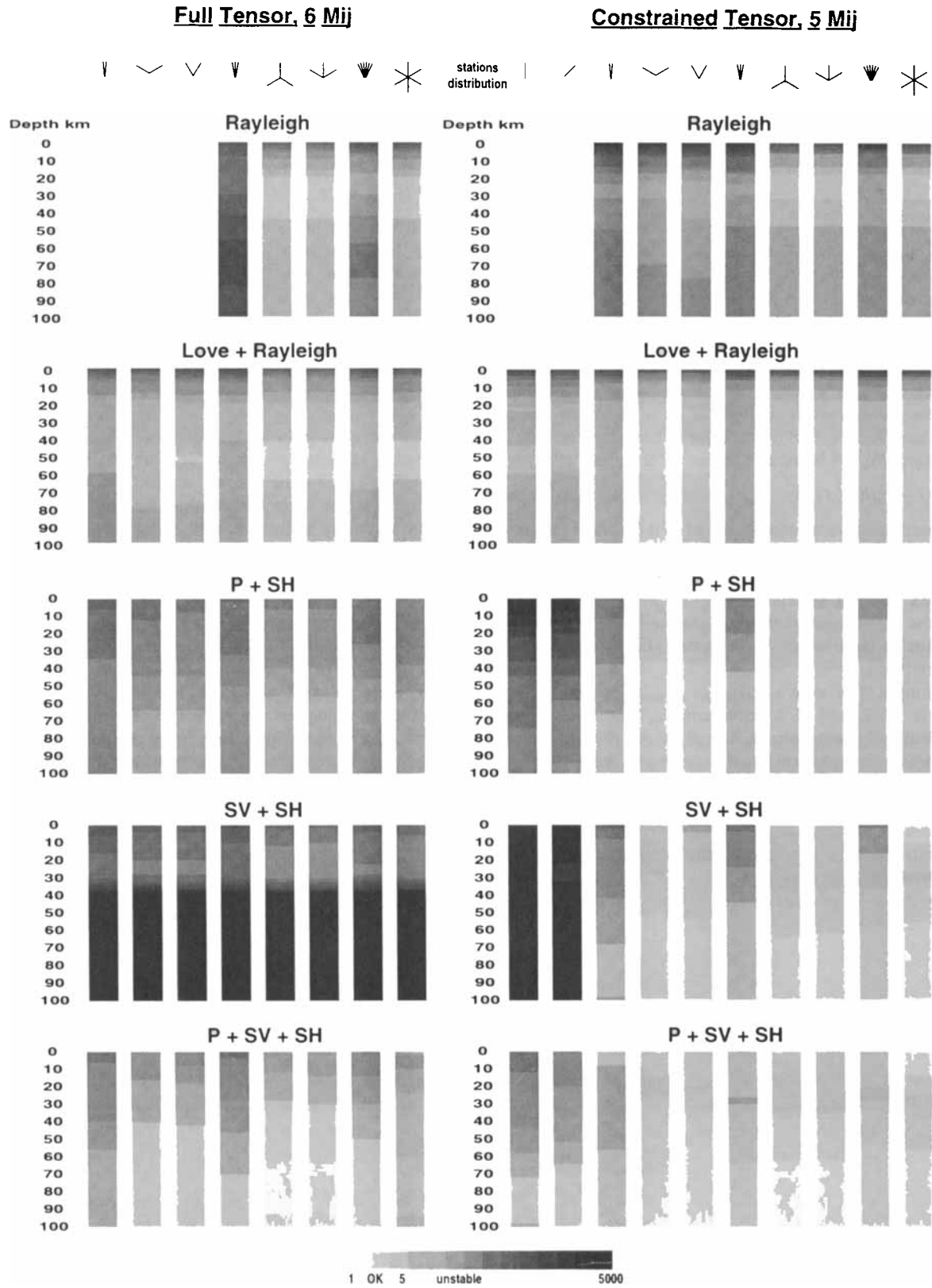


**Figure 2.** Tables of condition numbers of teleseismic moment tensor inversions, using different combinations of stations and components. The station distribution is symbolized on the top, and the grey scale codes the condition number as indicated at the bottom. The left part concerns full moment tensor inversions, the right part deviatoric ones. The values of the condition number are indicated for depths of 0–100 km. The period range is 10–60 s for body waves and 30–300 s for surface waves.

because of the poor resolution of  $M_{zz}$  with depth (Fitch *et al.* 1981). Other problems restricted to five unknowns can be solved with confidence from the mathematical point of view. As shown, for example, in Fig. 3, there are, for particular distributions of stations, safer ways of writing the condition  $M_{xx} + M_{yy} + M_{zz} = 0$ : eliminating either  $M_{xx}$  or  $M_{yy}$  gives a better conditioning.

### 3.2 Damping

Reducing the number of unknowns is probably the most efficient way to stabilize an ill-conditioned problem, but one might also investigate other procedures, e.g. by choosing appropriate data (inverting displacement, velocity or acceleration spectra for example), optimizing the signal-to-noise ratio, or even changing the parametrization (Dufumier & Cara 1995).

Another common procedure used to reduce conditioning instabilities, known as the 'Levenburg–Marquardt inverse' or 'damped least squares', is to introduce a damping factor  $\theta^2$  in the inversion. Eq. (9) becomes (Tarantola & Valette 1982)

$$\mathbf{M} = (\mathbf{G}^t \mathbf{G} + \theta^2 \mathbf{Id})^{-1} \mathbf{G}^t \mathbf{D}. \quad (10)$$

The damping factor  $\theta^2$  can be related to the *a priori* standard errors  $\sigma$  on the data and on the model ( $\theta^2 = \sigma_d^2 / \sigma_m^2$ ) and is usually used to eliminate the instabilities due to the lowest eigenvalues of  $\mathbf{G}^t \mathbf{G}$  (Menke 1989). As a consequence, the rank of the system solved by the data has to be reduced by the number of eigenvalues  $\lambda_i$  eliminated (Lévêque, Rivera & Wittlinger 1993).

For example, if we note  $\lambda_1 \leq \lambda_2 \leq \dots \leq \lambda_6$  the eigenvalues of the matrix  $\mathbf{G}^t \mathbf{G}$ , and if  $\theta^2$  eliminates  $\lambda_1$  but not  $\lambda_2$ , five independent unknowns can be solved. More precisely, if  $m_1$  is the eigenvector associated to  $\lambda_1$ , and  $m_0$  is the solution of the stable subsystem of rank five, we get a line of solutions  $M = m_0 + km_1$  in the 6-D space.

This does not eliminate *a priori* tensors including an isotropic component, and even if it restricts the population of possible tensors, it also leaves one degree of freedom in the solution. Similarly, if two eigenvalues were very small and eliminated

by the damping, only a tensor of degree four could be reliably solved, giving a plane of possible tensors.

### 3.3 Resolution

More information can be deduced from the resolution matrix (Tarantola 1987)

$$\mathbf{R} = (\mathbf{G}^t \mathbf{G} + \theta^2)^{-1} \mathbf{G}^t \mathbf{G}. \quad (11)$$

On its diagonal appear the resolutions of each moment tensor element (Fig. 4, left):  $R_{ii} = 0$  indicates that  $M_i$  is not solved at all,  $R_{ii} = 1$  that it is perfectly determined by the data.

The average number of parameters solved by the data is therefore given by the trace of the resolution matrix:

$$\text{Tr}(\mathbf{R}) = \sum_{i=1}^6 \frac{\lambda_i}{\lambda_i + \theta^2}. \quad (12)$$

We can deduce from this equation a limit on the damping allowing at least five parameters out of six to be solved, by developing it to the second order (this supposes that the damping factor is much lower than the third lowest eigenvalue, but if not, only a tensor of rank 3 could be solved):

$$\frac{\lambda_1}{\lambda_1 + \theta^2} + \frac{\lambda_2}{\lambda_2 + \theta^2} + 4 \geq 5,$$

i.e.

$$\theta^2 \leq \sqrt{\lambda_1 \lambda_2}. \quad (13)$$

The resolution matrices in Fig. 4 illustrate the influence of the damping on the average resolution of teleseismic surface-wave moment tensor inversions. On top, we use a strong damping (10 per cent of the largest eigenvalue), which eliminates largely the two lowest eigenvalues and gives consequently a rather poor average resolution: 0.63, equivalent to a proportion of four parameters on six. On the bottom matrix, we used a damping of 1 per cent, which eliminates only one eigenvalue and gives a better average resolution of 0.82, i.e. an average of five resolved parameters out of six.

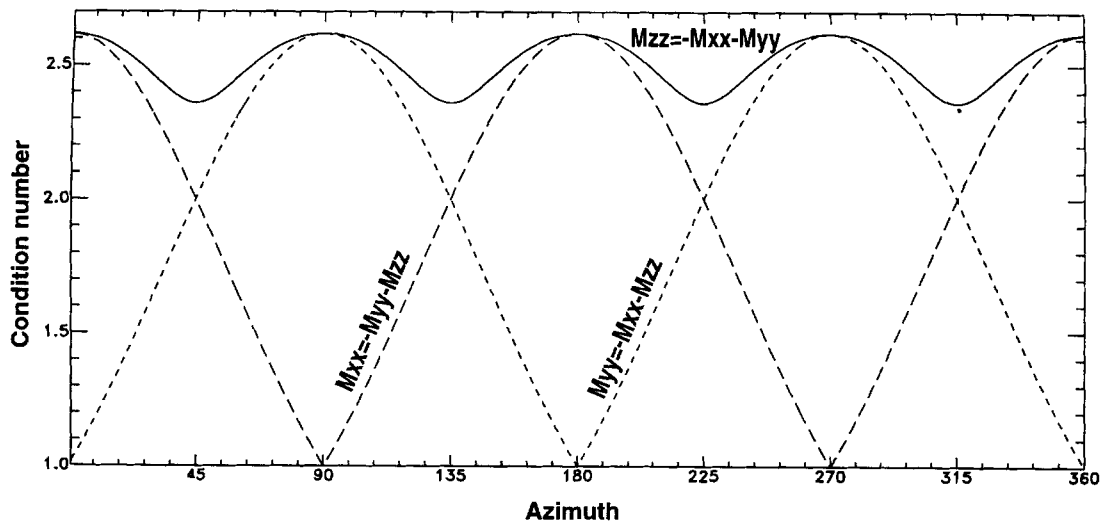
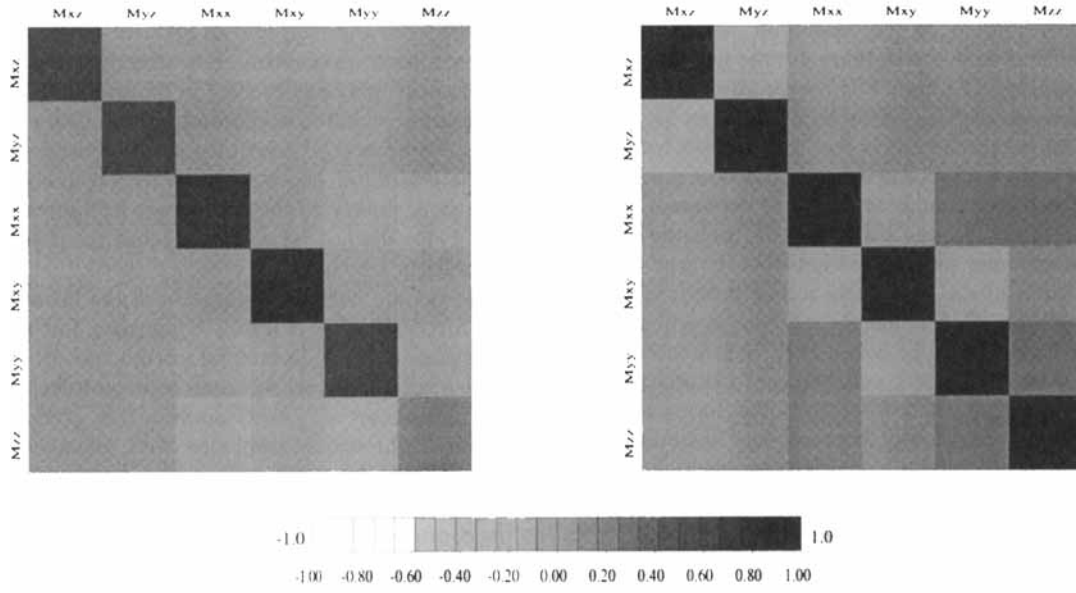


Figure 3. Azimuthal variation of the condition number of the single-station inverse problem, for three different formulations of the condition  $M_{xx} + M_{yy} + M_{zz} = 0$ .

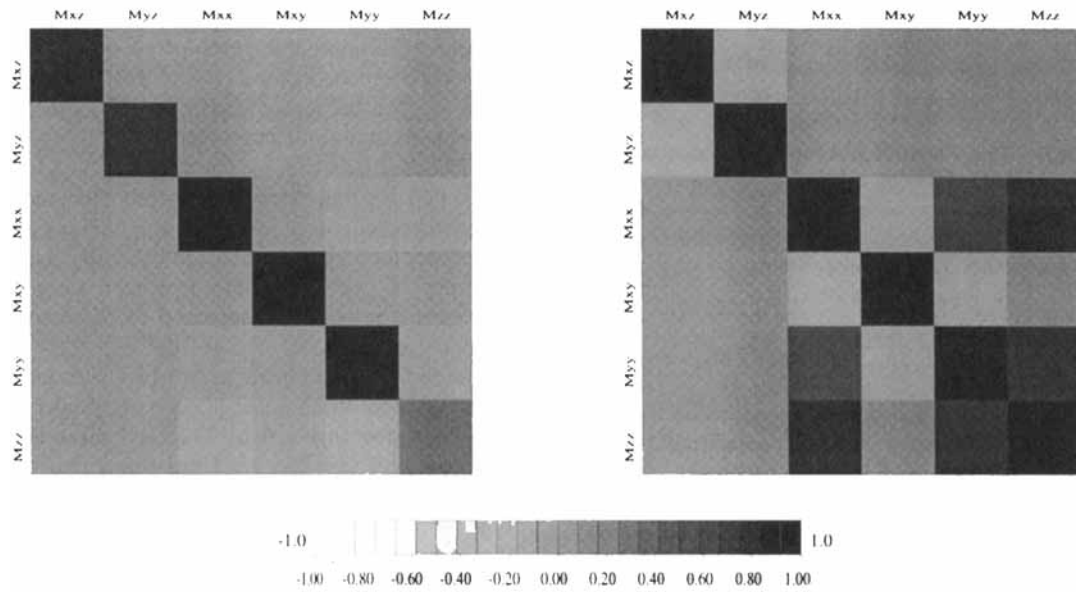
**Damped Least Squares At Exact Depth and Source Duration**



**Resolution Matrix**

**Correlation Matrix**

**Damped Least Squares with Shift in Depth and Source Duration**



**Resolution Matrix**

**Correlation Matrix**

**Figure 4.** Left: resolution matrices; the diagonal shows the resolution of each moment tensor element. Right: correlation matrices, showing the correlations or anticorrelations between the different  $M_{ij}$ . Full moment tensor inversions of surface waves are presented. On top, the inversion is performed with exact source depth and source duration, and using a damping of 10 per cent. Below, inversions are performed with a damping of 1 per cent, and include a slight error on the source depth and on the source duration. Interpretation is given in the text.

Downloaded from https://academic.oup.com/gji/article/131/3/595/2140391 by CNRS - ISTO user on 14 June 2021

### 3.4 Correlations and trade-offs

Looking in more detail at the matrices of Fig. 4, we can examine the distribution of the resolution of the moment tensor elements and their correlations. On the top figures, the different  $M_{ij}$  appear to be quite homogeneously resolved, and almost uncorrelated, whereas on the bottom figures,  $M_{zz}$  is the unique unsolved parameter and is strongly coupled with  $M_{xx}$  and  $M_{yy}$ . This is due to the fact that the first inversion is run for a synthetic configuration at exact source depth and source duration, while in the second case we ran the inversion with a slight shift in depth and source duration from the true model. This misestimation of the depth and source time function is systematically reflected as a strong correlation between the elements of the isotropic component, and among these elements  $M_{zz}$  appears to be particularly poorly solved in surface-wave inversions, especially at shallow depths. This formalizes the trade-offs observed empirically between the isotropic part, the hypocentral depth and the source time function (Fitch *et al.* 1981; Stein & Wiens 1986). It also indicates that, when an additional constraint must be applied in order to reduce the number of unknowns from six to five, choosing a constraint on the isotropic part, and particularly the condition  $M_{zz} = -M_{xx} - M_{yy}$ , is among the best possible choices.

Another illustration of the trade-off between the isotropic component and the hypocentral depth and source duration is given in Fig. 5. This application concerns a surface-wave inversion, using five three-component stations and periods from 35 to 300 s. The linear inversion for the moment tensor is performed on each point of a grid in depth and source duration, illustrating the non-linear dependence of the global inversion on these source parameters. The correct source mechanism, indicated by stars, is retrieved at the exact source depth and duration. The deviatoric part of the mechanism remains stable all over the grid, while the isotropic component appears to be a pure artefact of errors in depth and source duration. An additional trade-off can be noted concerning the seismic moment, which varies by a factor of 20 over the grid.

The same trade-offs can be observed for body waves, except that the deviatoric mechanism and the seismic moment remain stable on a small zone only (Dufumier 1996).

## 4 APPLICATION TO REGIONAL WAVEFORM INVERSIONS

We have presented in the second part some limitations on the resolution of a full moment tensor appearing in teleseismic inversions, where  $P$ ,  $S$  and surface waves can be easily separated. The question of mixing various data sets together, especially at regional scale, and of its effect on the non-double-couple part of the mechanism has been discussed by several authors. Kuge & Lay (1994a) note the dependence of the non-double-couple component on the type of inversion used (only body waves or combined body waves and surface waves). Pearce & Rogers (1989) note bias in the estimation of the isotropic component when  $P$  and  $S$  waves are used together, for example in full waveform inversion, due to the dominance of the  $S$  over the  $P$  amplitudes, whereas only the  $P$  waves carry information on the isotropic part.

Therefore, even if more information is available in full waveforms than in isolated groups of waves, some methodological precautions are also required in waveform inversions.

This is emphasized by the fact that most regional inversions are non-linear, including the relocalization of the event or the precise determination of the rupture complexity, so that trade-offs between the isotropic component and other parameters become hard to control. For example, spurious isotropic components may be observed in time-variable moment tensor inversions, when the resolution of the source history becomes poor (Campus *et al.* 1996). In such applications, an analysis of the resolution of the moment tensor components at each time step, similar to the one shown in Section 3.4, might be useful to discard spurious volumetric parts due to an insufficient resolution.

We present here an application of the theory developed in the first part of two results concerning full moment tensor inversions for the Roermond earthquake (the Netherlands, 1992 April 13,  $M_w = 5.4$ ), using regional waveforms.

Dufumier *et al.* (1997) studied this earthquake using a Monte-Carlo search combined with an inversion for time-variable moment rate functions  $\dot{M}_{ij}(t)$ , from which is extracted afterwards the average tensor  $M_{ij}$ . Although only the result of the constrained inversion for a deviatoric tensor was published, we present here the corresponding result of the full moment tensor inversion (Fig. 6a). The deviatoric part is very similar to the constrained solution, with  $\epsilon = 35$  per cent of non-double-couple part, corresponding to an angle  $\alpha = 39^\circ$  between the dislocation and the normal to the fault plane. In addition, we observed 14 per cent of isotropic component in compression ( $I = +7.6 \times 10^{16}$  N m). Supposing reasonably that this event is tectonic, this isotropic component would correspond to a ratio  $\lambda/\mu$  of  $-0.45$ , and should therefore be considered spurious. Following our new approach, supposing that this event might include also a non-tectonic mechanism, such as fluid intrusion, we can determine the parts of tectonic and non-tectonic isotropic components for a given ratio  $\lambda/\mu$ . Considering a ratio  $V_p/V_s = \sqrt{3}$  at the source ( $\lambda = \mu$ ), the full moment tensor would correspond to a non-tectonic implosion  $E = -5.2 \times 10^{17}$  N m, compensated by a tectonic compression  $I - E = 5.9 \times 10^{17}$  N m. These two isotropic components are as energetic as the tectonic seismic moment itself ( $M_0 = 5.6 \times 10^{17}$  N m) and are clearly unrealistic for an earthquake. On this basis also, we can affirm that the 14 per cent of the isotropic component observed here, which might have appeared to be reasonably small, is definitely spurious.

The second full moment tensor inversion published for this event is from Braunmiller, Dahm & Bonjer (1994), whose result is shown in Fig. 6(b). The mechanism is almost a pure double-couple ( $\alpha = 88^\circ$ ,  $\epsilon = 3$  per cent), plus again about 15 per cent of isotropic compression ( $I = +1.4 \times 10^{16}$  N m). At that time, this component could be considered to belong to the tectonic process, since it would correspond to a ratio  $\lambda/\mu$  of 3, possibly realistic ( $V_p/V_s = 2.2$ ). Even considering a more reasonable ratio  $\lambda/\mu = 1$ , the non-tectonic and the tectonic isotropic parts would be both around  $+7 \times 10^{15}$  N m, e.g. only 8 per cent of the total seismic moment each. Therefore the small compression observed in this earthquake mechanism cannot be rejected here on a realism criterion.

The comparison of these two examples is illustrative, since they contained *a priori* the same amount of isotropic component, but considering the necessary compatibility with the rheology of the source, one appears to be definitely spurious while the second one cannot be rejected.

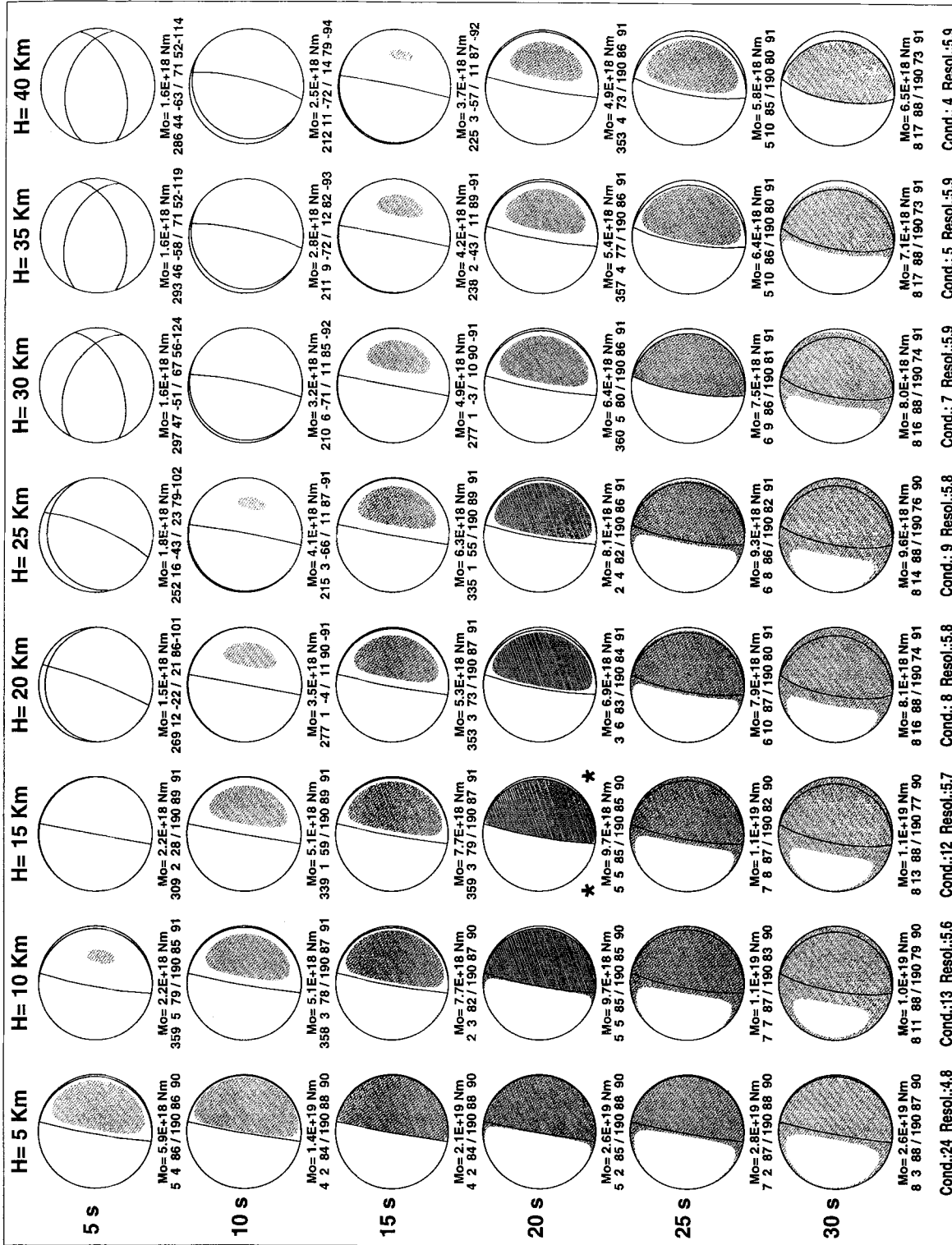
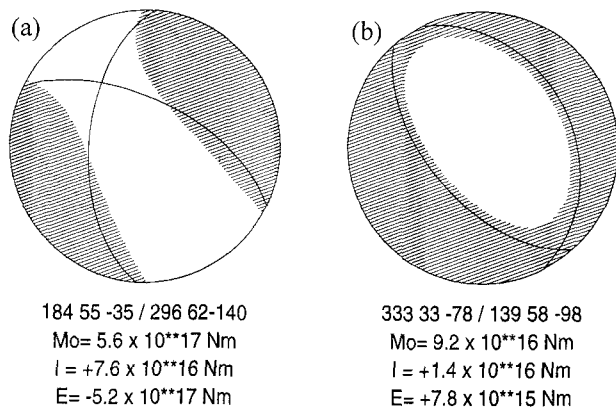


Figure 5. An example of iterative moment tensor inversion on a grid in depth (horizontally) and source duration (vertically), using teleseismic Love and Rayleigh waves of five stations. The exact source is indicated by stars. The gray intensity of the mechanism is proportional to the variance reduction, and its seismic moment and the strike, dip and rake angles of the best nodal planes are reported below. The resolution and the condition number are indicated for each depth.



**Figure 6.** Full moment tensor inversions for the Roermond (1992 April 13) earthquake, after (a) Dufumier *et al.* (1997) and (b) Braunmiller *et al.* (1994). The respective tensors are, in Aki & Richards' (1980) conventions ( $x$ , north;  $y$ , east;  $z$ , down): (a)  $M_{xx} = 1.68 \times 10^{16}$ ,  $M_{xy} = 44.77 \times 10^{16}$ ,  $M_{xz} = 12.50 \times 10^{16}$ ,  $M_{yy} = 48.13 \times 10^{16}$ ,  $M_{yz} = 0.56 \times 10^{16}$ ,  $M_{zz} = -26.94 \times 10^{16}$  Nm; (b)  $M_{xx} = 3.86 \times 10^{16}$ ,  $M_{xy} = 4.14 \times 10^{16}$ ,  $M_{xz} = -3.03 \times 10^{16}$ ,  $M_{yy} = 7.08 \times 10^{16}$ ,  $M_{yz} = -2.48 \times 10^{16}$ ,  $M_{zz} = -6.71 \times 10^{16}$  Nm. The radiation of the tensor is shown in the projection of Schmitt on the lower hemisphere, together with the nodal planes of the best double-couple, whose strike, dip and rake angles are indicated below.  $M_0$  is the seismic moment of the deviatoric tensor, following Dziewonski *et al.* (1981),  $I$  is the observed volumetric variation ( $\text{Trace}(\mathbf{M})/3$ ), and  $E$  the non-tectonic part of  $I$ , as described in the text.

## 5 SYNTHESIS AND IMPROVEMENTS

Synthesizing the various aspects of this study on the resolvability of the isotropic component, we now propose some improvements to the inverse problems which do not allow for full moment tensor retrieval.

We have seen in the first part that the physical model classically used to describe moment tensors for tectonic events imposes a compatibility constraint between the isotropic component and the Earth's rheology. When the moment tensor is considered as the representation of a tectonic event occurring as an arbitrary slip near a fault plane, it is necessary to check the reliability of the ratio  $\lambda/\mu$  associated with the observed isotropic component. An alternative is to impose a constraint on the moment tensor in order to describe it by only five independent physical parameters. Among such models are the deviatoric tensors but not the combinations of a double-couple plus a volumetric component. However, if one wants to consider all the information contained in a full moment tensor, then another physical parameter should be added to the tectonic model, which can be, advantageously, a second volumetric component of non-tectonic origin (e.g. explosion, pore pressure drop). A wide range of phenomena can be explained by this unique model, such as pure shear dislocations, pure explosions, non-double-couple deviatoric tensors, off-fault tectonic slips, nuclear explosions and associated spall and stress release, tensile crack openings, fluid or magma intrusions, etc. An application of this model to two regional waveform inversions exhibiting *a priori* similar isotropic parts shows that an analysis in terms of tectonic and non-tectonic volumetric variations is essential for a pertinent interpretation of the isotropic component.

The second critical analysis which has been carried out is

from the mathematical point of view, since many methods offer poorly controlled results, whose careless interpretation might be misleading. For example, teleseismic surface-wave and body-wave full moment tensor inversions appear to be ill-conditioned, whatever the distribution of stations used, while deviatoric moment tensor inversions are stable when using at least two stations separated by  $60^\circ$  in azimuth.

When damping is used to stabilize the inversion, attention should be paid to the fact that fewer parameters can be solved (the number being easily deduced from the computation of the eigenvalues of the problem). In particular, a limit on the damping has been defined which allows us to solve five elements of the tensor out of six. Then the tensor becomes non-unique, but may be chosen from a line of solutions in the 6-D space.

Therefore, the constraint to be applied on the moment tensor is not necessarily zero volumetric variation. The less controlled parameter(s) can simply be fixed, limiting the space of the solutions to certain particular types of mechanisms: for example, Kanamori & Given (1981) proposed setting  $M_{xz} = M_{yz} = 0$  at shallow depths and long periods, inverting for pure strike-slips or dip-slips. Such a simple linear constraint can be easily chosen looking to the relative resolution of the different parameters in the resolution matrix. It appears for example, that in teleseismic linear moment tensor inversions, a constraint on the isotropic component is most desirable (and particularly on  $M_{zz}$  when using surface waves). In non-linear approaches, attention should be paid to the dependence of the isotropic component on the estimation of the depth and on the source time function.

Among other possible constraints, reducing the number of parameters from six to five, Ekström & Richards (1994) suggested inverting for a double-couple plus an isotropic mechanism, a suitable choice for the study of nuclear explosions. This direct procedure is not linear, but a linearized two-step procedure can be proposed, thanks to the remaining degree of freedom. First, we invert linearly for a stable tensor  $m_0$  of rank five, a procedure that can be safely damped, considering only the five greatest eigenvalues. Then any tensor  $m_0 + km_1$  is a solution,  $m_1$  being the eigenvector associated with the sixth, eliminated, eigenvalue  $\lambda_1$ . Following this direction of error, the deviatoric part of the tensor is projected on the subspace of the double-couples (Fig. 7), solving the condition of a zero determinant (which may give up to three solutions):

$$\det \left[ (m_0 + km_1) - \frac{1}{3} \text{Tr}(m_0 + km_1) \mathbf{Id} \right] = 0. \quad (14)$$

A similar method of projection can be proposed, in order to obtain a full moment tensor compatible with both a tectonic model and the Earth's rheology. As before, we invert for a stable five-parameter moment tensor  $m_0$ , considering only the subsystem of the five greatest eigenvalues, and compute the sixth eigenvector  $m_1$ . Then we search for the full tensor  $m_0 + km_1$  corresponding to a given  $\lambda/\mu$  ratio. For example, if we suppose  $\lambda = \mu$ , we search for the unique value of  $k$  giving

$$(m_0 + km_1)_{\langle P, N, T \rangle} = \mu SD \begin{pmatrix} 2 \cos \alpha - 1 & 0 & 0 \\ 0 & \cos \alpha & 0 \\ 0 & 0 & 2 \cos \alpha + 1 \end{pmatrix}. \quad (15)$$

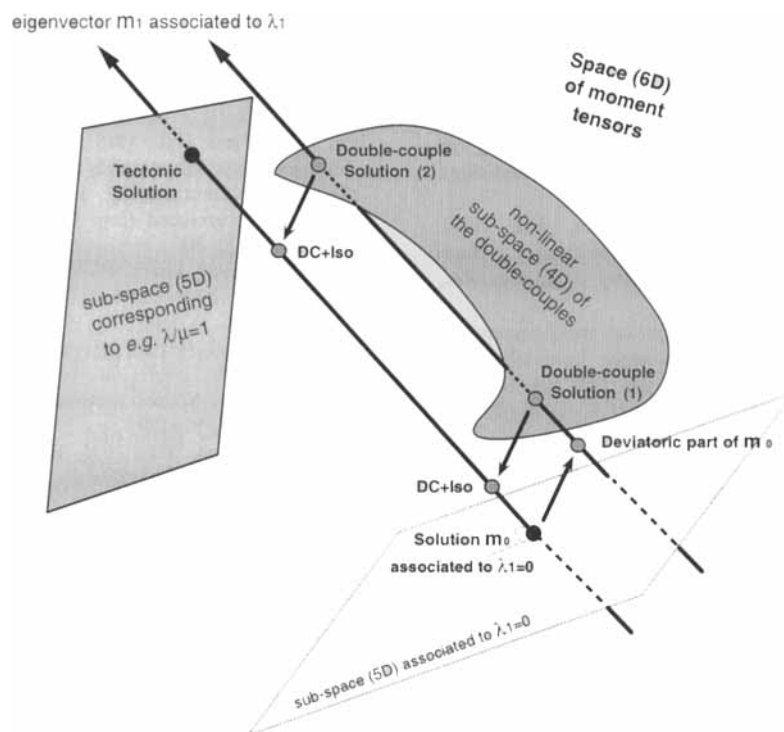


**Figure 7.** Schematic illustration of the procedures described in Section 5 to obtain reliable constrained moment tensors. The full space of parameters is 6-D and the surfaces represent 5-D or 4-D subspaces. An initial reliable solution is obtained using the subsystem of the five greatest eigenvalues. Then the solution can be projected onto the subspace of the tectonic moment tensors, following the line of possible solutions given by the eigenvector  $m_1$  associated to the lowest eigenvalue  $\lambda_1$  (black dots). Alternatively, the deviatoric part of the initial tensor can be projected onto the subspace of the double-couples, in order to obtain finally the sum of a double-couple and of an isotropic mechanism (grey dots).

Let us note also that similar procedures can be used to solve much more ill-conditioned problems, such as single-station inversions, or surface-wave moment tensor inversions for superficial events. In these cases, only four parameters of the moment tensor can be solved: for example, an initial deviatoric tensor can be obtained linearly and then projected onto the space of the double-couples.

Without referring to constraining ‘exact’ conditions, one may prefer to find a tensor that ‘best’ fits a given model. Julian (1986) proposed such an approach, relying on linear programming methods, minimizing or maximizing a given function. For example, one can search for the most thrust-like, the most strike-slip-like or the most explosion-like mechanism, or the one achieving the best fit with some polarities.

## 6 CONCLUSION

We have presented several approaches which show that the interpretation of full moment tensors, and in particular their isotropic component, should be subject to caution. First, the classical tectonic model used to describe earthquake moment tensors may lead to isotropic components incompatible with the Earth’s rheology. We show that considering the trace of the observed moment tensor as the expression of a unique volumetric variation at the source is misleading, and that a decomposition in tectonic and non-tectonic isotropic components is more reliable and informative. This extended model allows us to explain most types of geophysical sources without facing physical restrictions.

Concerning the inverse problem leading to the moment tensor, it appears that a constraint on the moment tensor is

most often needed. First, teleseismic surface-wave and body-wave inversions are too poorly conditioned to allow for the direct retrieval of a full moment tensor, and constraining the isotropic part appears to be a particularly suitable choice. Second, when applying damping in the inversion, the solution becomes non-unique. Taking advantage of this, the solution can be projected onto a preferred set of solutions, such as the combination of an explosion and a double-couple, or a ‘tectonic’ tensor, whose direct determination could not be achieved linearly.

## ACKNOWLEDGMENTS

During the course of this work, HD benefited from a BDI-PhD grant from CNRS, at URA 1358 of CNRS, Laboratoire de Sismologie–Université Louis Pasteur de Strasbourg. This work was completed under Human Capital and Mobility contract of the European Commission, no. ERBCHBGCT940645, at the Dipartimento di Scienze della Terra–Università di Trieste.

## REFERENCES

- Aki, K. & Richards, P.G., 1980. *Quantitative Seismology, Theory and Methods*, W. H. Freeman, San Francisco.
- Braunmiller, J., Dahm, T. & Bonjer, K.P., 1994. Source mechanism of the 1992 Roermond earthquake from surface-wave inversion of regional data, *Geophys. J. Int.*, **116**, 663–672.
- Campus, P., Suhadolc, P., Panza, G.F. & Sileny, J., 1996. Complete moment tensor retrieval for weak events: application to orogenic and volcanic areas, *Tectonophysics*, **261**, 147–163.
- Doornbos, D.J., 1982. Seismic moment tensors and kinematic source parameters, *Geophys. J. R. astr. Soc.*, **69**, 235–251.

- Dufumier, H., 1996. On the limits of linear moment tensor inversions of teleseismic body wave spectra, *Pageoph*, **147**, 467–482.
- Dufumier, H. & Cara, M., 1995. On the limits of linear moment tensor inversions of surface wave spectra, *Pageoph*, **145**, 235–257.
- Dufumier, H., Michelini, A., Du, Z., Bondar, I., Sileny, J., Mao, W., Kravanja, S. & Panza, G.F., 1997. Regional structure modelling and source inversion for the 1992 Roermond earthquake, *J. Seismology*, in press.
- Dziewonski, A.M., Chou, T.A. & Woodhouse, J.H., 1981. Determination of earthquake source parameters from waveform data for studies of global and regional seismicity, *J. geophys. Res.*, **86**, 2825–2852.
- Ekström, G. & Richards, P.G., 1994. Empirical measurements of tectonic moment release in nuclear explosions from teleseismic surface waves and body waves, *Geophys. J. Int.*, **117**, 120–140.
- Fitch, T.J., North, R.G. & Shields, M.W., 1981. Focal depths and moment tensor representations of shallow earthquakes associated with the great Sumba earthquake, *J. geophys. Res.*, **86**, 9357–9374.
- Foulger, G. & Long, R., 1984. Anomalous focal mechanisms: tensile crack formation on an accreting plate boundary, *Nature*, **310**, 43–45.
- Frolich, C., Riedesel, M.A. & Apperson, K.D., 1989. Note concerning possible mechanisms for non-double-couple earthquake sources, *Geophys. Res. Lett.*, **16**, 523–526.
- Hara, T., Kuge, K. & Kawakatsu, H., 1996. Determination of the isotropic component of deep focus earthquakes by inversion of normal-mode data, *Geophys. J. Int.*, **127**, 515–528.
- Hudson, J.A., Pearce, R.G. & Rogers, R.M., 1989. Source type plot for inversion of the moment tensor, *J. geophys. Res.*, **94**, 765–774.
- Jost, M.L. & Herrmann, R.B., 1989. A student's guide to and review of moment tensors, *Seism. Res. Lett.*, **60**, 37–57.
- Julian, B.R., 1986. Analysing seismic-source mechanism by linear-programming methods, *Geophys. J. R. astr. Soc.*, **84**, 431–443.
- Kanamori, H. & Stewart, G., 1976. Mode of the strain release along the Gibbs Fracture Zone, Mid-Atlantic Ridge, *Phys. Earth planet. Inter.*, **11**, 312–332.
- Kanamori, H. & Given, J.W., 1981. Use of long-period surface waves for rapid determination of earthquake source parameters, *Phys. Earth planet. Inter.*, **27**, 8–31.
- Kawakatsu, H., 1989. Centroid single force inversion of seismic waves generated by landslides, *J. geophys. Res.*, **94**, 12 363–12 374.
- Kawakatsu, H., 1996. Observability of the isotropic component of a moment tensor, *Geophys. J. Int.*, **126**, 525–544.
- Knopoff, L. & Randall, M.J., 1970. The compensated linear-vector dipole: a possible mechanism for deep earthquake, *J. geophys. Res.*, **75**, 4957–4963.
- Kuge, K. & Lay, T., 1994a. Data-dependent non-double-couple components of shallow earthquake source mechanisms: effects of waveform inversion instability, *Geophys. Res. Lett.*, **21**, 9–12.
- Kuge, K. & Lay, T., 1994b. Systematic non-double-couple components of earthquake mechanisms: the role of fault zone irregularity, *J. geophys. Res.*, **99**, 15 457–15 467.
- Lanczós, C., 1961. *Linear Differential Operators*, Ch. 3, Van Nostrand, London.
- Langston, C.A., Barker, J.S. & Pavlin, G.B., 1982. Point source inversion techniques, *Phys. Earth planet. Inter.*, **30**, 228–241.
- Lévêque, J.J., Rivera, L. & Wittlinger, G., 1993. On the use of the checker-board test to assess the resolution of tomographic inversions, *Geophys. J. Int.*, **115**, 313–318.
- Mendiguren, J.A., 1977. Inversion of surface wave data in source mechanism studies, *J. geophys. Res.*, **82**, 889–894.
- Menke, W., 1989. Geophysical data analysis: discrete inverse theory (revised edition), *International Geophysics Series*, **45**, pp. 119–125, Academic Press, Harcourt Brace Jovanovitch.
- Pearce, R.G. & Rogers, R.M., 1989. Determination of earthquake moment tensors from teleseismic relative amplitude observations, *J. geophys. Res.*, **94**, 775–786.
- Satake, K., 1985. Effects of station coverage on moment tensor inversion, *Bull. seism. Soc. Am.*, **75**, 1657–1667.
- Silver, P.G. & Jordan, T.H., 1982. Optimal estimation of scalar seismic moment, *Geophys. J. R. astr. Soc.*, **70**, 755–787.
- Sipkin, S.A., 1986. Interpretation of non-double-couple earthquake mechanisms derived from moment tensor inversion, *J. geophys. Res.*, **91**, 531–547.
- Stein, S. & Wiens, D.A., 1986. Depth determination for shallow teleseismic earthquakes: methods and results, *Rev. Geophys.*, **24**, 806–832.
- Takei, Y. & Kumazawa, M., 1994. Why have the single force and torque been excluded from the seismic source model?, *Geophys. J. Int.*, **118**, 20–30.
- Tarantola, A., 1987. *Inverse Problem Theory, Methods for Data Fitting and Model Parameter Estimation*, Elsevier, Amsterdam.
- Tarantola, A. & Valette, B., 1982. Generalised non-linear inverse problem solved using the least-squares criterion, *Rev. Geophys. Res.*, **74**, 6603–6661.
- Udias, A., 1991. Source mechanism of earthquakes, *Advances in Geophysics*, **33**, 81–139.
- Wu, Z.L. & Chen, Y.T., 1996. Decomposition of seismic moment tensors for underground nuclear explosions, *Pageoph*, **147**, 357–366.

## APPENDIX A: RELATING A MOMENT TENSOR TO SIX INDEPENDENT PHYSICAL PARAMETERS

We provide here the equations relating uniquely a symmetric moment tensor  $\mathbf{M}$  to the six independent parameters of the model proposed in Section 2.2, i.e. the vectors  $\mathbf{n}$ ,  $\mathbf{s}$  and the amounts of energy release  $SD$  and  $E$ .

The isotropic and deviatoric parts of  $\mathbf{M}$  are, respectively,

$$\mathbf{I} = \frac{1}{3} \text{Trace}(\mathbf{M}) \mathbf{Id} = \left[ \left( \lambda + \frac{2}{3} \mu \right) (\mathbf{s} \cdot \mathbf{n}) SD + E \right] \mathbf{Id}, \quad (\text{A1})$$

$$\mathbf{Dev} = \mathbf{M} - \mathbf{I} = \mu SD \left( \mathbf{sn}^\perp + \mathbf{ns}^\perp - \frac{2}{3} (\mathbf{s} \cdot \mathbf{n}) \mathbf{Id} \right). \quad (\text{A2})$$

The normalized eigenvectors of the deviatoric part are

$$v_1 = \frac{\mathbf{n} + \mathbf{s}}{\|\mathbf{n} + \mathbf{s}\|}, \quad v_2 = \frac{\mathbf{n} \wedge \mathbf{s}}{\|\mathbf{n} \wedge \mathbf{s}\|}, \quad v_3 = \frac{\mathbf{n} - \mathbf{s}}{\|\mathbf{n} - \mathbf{s}\|},$$

and the corresponding eigenvalues are

$$v'_1 = \left( \frac{1}{3} (\mathbf{n} \cdot \mathbf{s}) + 1 \right) \mu SD, \quad v'_2 = -\frac{2}{3} (\mathbf{n} \cdot \mathbf{s}) \mu SD,$$

$$v'_3 = \left( \frac{1}{3} (\mathbf{n} \cdot \mathbf{s}) - 1 \right) \mu SD, \quad (v'_1 \geq v'_2 \geq v'_3, v'_1 > 0, v'_3 < 0).$$

Then

$$\mathbf{n} \cdot \mathbf{s} = \frac{-3v'_2}{v'_1 - v'_3} \quad \text{and} \quad SD = \frac{v'_1 - v'_3}{2\mu}. \quad (\text{A3})$$

$E$  is given by

$$E = \left[ \frac{1}{3} \text{Trace}(\mathbf{M}) - \left( \lambda + \frac{2}{3} \mu \right) (\mathbf{s} \cdot \mathbf{n}) SD \right] \mathbf{Id}, \quad (\text{A4})$$

and  $\mathbf{n}$  and  $\mathbf{s}$  are retrieved from

$$\begin{aligned} \mathbf{n} &= \frac{1}{2} [(\mathbf{n} + \mathbf{s}) + (\mathbf{n} - \mathbf{s})] \\ &= \frac{1}{\sqrt{2}} \left( \sqrt{(1 + \mathbf{n} \cdot \mathbf{s})} v_1 + \sqrt{(1 - \mathbf{n} \cdot \mathbf{s})} v_3 \right), \end{aligned} \quad (\text{A5})$$

$$\begin{aligned} \mathbf{s} &= \frac{1}{2} [(\mathbf{n} + \mathbf{s}) - (\mathbf{n} - \mathbf{s})] \\ &= \frac{1}{\sqrt{2}} \left( \sqrt{(1 + \mathbf{n} \cdot \mathbf{s})} v_1 - \sqrt{(1 - \mathbf{n} \cdot \mathbf{s})} v_3 \right). \end{aligned} \quad (\text{A6})$$